GEORGIA INSTITUTE OF TECHNOLOGY
OFFICE OF CONTRACT ADMINISTRATION

SPONSORED PROJECT TERMINATION

Posted CAH

Date: June 15, 1977

Project Title: A Kinetics Investigation of Reactions Involving Chlorine Containing Compounds

Project No: A-1886

Project Director: Drs. D. D. Davis and A. Ravishankara

Sponsor: NASA - Langley Research Center; Hampton, VA 23665

Effective Termination Date: 4/30/77

Clearance of Accounting Charges: 4/30/77

Grant/Contract Closeout Actions Remaining:

- _ Final Invoice and Closing Documents
- X Final Fiscal Report (NASA Form 1031 w/Final-Cumulative Cost Expenditure Report)
- X Final Report of Inventions
- X Govt. Property Inventory & Related Certificate
- _ Classified Material Certificate
- _ Other _____

has property - see cards

Assigned to: Applied Sciences Laboratory (School/Laboratory)

COPIES TO:

- Project Director
- Division Chief (EES)
- School/Laboratory Director
- Dean/Director—EES
- Accounting Office
- Procurement Office
- Security Coordinator (OCA)
- Reports Coordinator (OCA) ✓
- Library, Technical Reports Section
- Office of Computing Services
- Director, Physical Plant
- EES Information Office
- Project File (OCA)
- Project Code (GTRI)
- Other _____

CA—4 (3/76)

A KINETICS INVESTIGATION OF REACTIONS INVOLVING CHLORINE CONTAINING COMPOUNDS

Final Report

June 1, 1977

Submitted to

NASA Langley Research Center
Hampton, Virginia

Prepared by:

Dr. Douglas Davis

and

Dr. A. Ravishankara

Applied Sciences Laboratory
Georgia Institute of Technology
Atlanta, Georgia 30332

During the nine months of NASA grant (NSG-1322), we have obtained rate constant data for reactions of chlorine atoms with three stratospheric constituents, NO, NO_2, and SO_2." In addition, the absolute absorption cross-sections for three lines in the 9-0 band of the $A^2\Pi$-$X^2\Pi$ transition of the ClO radical have been measured. A detailed discussion on the rate data for the reactions,

$$Cl(^2P_{3/2}) + NO + M \longrightarrow ClNO + M \qquad (240\text{-}350K)$$

$$Cl(^2P_{3/2}) + NO_2 + M \longrightarrow ClNO_2 + M \qquad (240\text{-}350K)$$

$$Cl(^2P_{3/2}) + SO_2 + M \longrightarrow SO_2Cl + M \qquad 298K$$

is presented in Section A. Section B describes the work carried out on the ClO absorption cross-section measurements.

SECTION A

A kinetics study of the reactions of Cl atoms with NO, NO_2, and SO_2.

Introduction

Chlorine has now been established as a key reactive species in the stratosphere. The reaction of chlorine atoms with O_3 results in a depletion of ozone through the catalytic cycle,

$$Cl + O_3 \longrightarrow ClO + O_2$$

$$\underline{ClO + O \longrightarrow O_2 + Cl}$$

$$O + O_3 \longrightarrow 2O_2 \quad .$$

The chain length of this cycle is controlled to a very large extent by other constituents of the stratosphere (CH_4, HO_2, H_2, etc.), which react with chlorine atoms, thereby temporarily "tying up" this species in an inactive form. In addition to the above catalytic cycle, reactions involving NO_x also deplete ozone. Recently, however, the ClO radical has been shown to react with NO_2 to form an inactive species, $ClONO_2$. Thus, this reaction couples ClO_x chemistry with NO_x chemistry, and represents a short term sink for both active species.

To further our understanding of such sink processes which relate the ClO_x cycle to the NO_x cycle, we have examined the reactions of Cl atoms with NO and NO_2 , i.e.,

$$\text{(a)} \quad Cl(^2P_{3/2}) + NO \xrightarrow{M} ClNO$$

$$\text{(b)} \quad Cl(^2P_{3/2}) + NO_2 \xrightarrow{M} ClNO_2 \ .$$

In addition to the above processes, we have also investigated a totally new sink reaction involving the sulfur species, SO_2 . The latter study was initiated, in part, due to the recently reported SO_2 results

of Sagawa and Itoh (1976). Measurements by these authors suggest stratospheric SO_2 levels in the parts per million range. Hence, we have studied the reactions of Cl atoms with SO_2,

$$(c) \quad Cl(^2P_{3/2}) + SO_2 \xrightarrow{M} ClSO_2$$

to explore the possibility that the product of this reaction might act as a sink for Cl atoms.

Experimental

In this investigation of reactions (1), (2), and (3), the well-established technique of flash photolysis-resonance fluorescence was used. A complete description of the system (Davis, *et al.*, 1974, 1972a, 1972b) and the specific experimental procedures for studying Cl atom reactions (Watson, *et al.*, 1976) have been published elsewhere. Hence, in this report, we have pointed out only those features unique to the present study.

In this investigation, a Pyrex cell with an internal volume of $\sim 150 cm^3$ was employed. The reaction mixture was maintained at a known constant temperature by circulating either methanol (240-300K) or silicone oil (350K) from a thermostated circulating bath through the outer jacket of a reaction cell. The temperature of the reaction cell was measured with an iron-constantan thermocouple. The photolysis of either 10μ of CCl_4 or 25μ of $CF_2ClCFCl_2$ was used to produce Cl atom concentrations of $\sim 10^{10}$ cm^{-3}. All three reactions were studied under pseudo-first order conditions, with the concentrations of the stable reactants (NO, NO_2, or SO_2) in large excess.

Results

The results for the $Cl + NO$, and $Cl + NO_2$ study are shown in Tables I and II. At each temperature and diluent gas pressure, the bimolecular rate constants (k_a, k_b', and k_c) were computed from measured pseudo-first order rate constants using a linear least square analysis. The quoted errors for each k_{bi} are 2σ. The values of k_{bi} were measured as a function of pressure for two diluent gases, He and N_2. Plots of k_{bi} vs pressure, for reactions (a) and (b), are shown in Figures 1 and 2. In addition, the dependence of $\ln k_{ter}$ vs $1/T$, for reactions (a) and (b), are shown in Figures 3 and 4. A least square analysis of the temperature data on reactions (1) and (2) gave:

$$k_{a(ter)} = 1.63 \times 10^{-33} e^{(1186/T)} \quad \text{for M = He},$$

and

$$k_{b(ter)} = 1.45 \times 10^{-31} e^{(529/T)} \quad \text{for M = He}$$

$$= 3.42 \times 10^{-31} e^{(460/T)} \quad \text{for M = } N_2 .$$

At room temperature, the $Cl + SO_2 + M$ reaction did not proceed to a measurable extent until the total pressure of the nitrogen diluent gas was increased to 500 torr. Even under these high pressure conditions, the bimolecular rate constant was only $\sim 1.5 \times 10^{-15}$. We also observed that a plot of the pseudo-first order rate constant k_c' vs $[SO_2]$ was non-linear, probably indicating that SO_2 is a more efficient third body than N_2. We have estimated the value of $k_{c(N_2)}$ to be $\sim 9 \times 10^{-35}$ based on the linear initial part of the k' vs $[SO_2]$ plots.

Discussion

$$(i)\quad Cl(^2P_{3/2}) + NO \xrightarrow{M} ClNO$$

As shown in Figure 1, k_a'' at 298K increases linearly with the pressures of both N_2 and He . The linearity of the plots indicates that this reaction is truly termolecular at the pressures studied. Also, we find N_2 to be a better third body than He ; the efficiency ratio is 1.4 . Only one value of k_a has been reported in the literature (Clark, Clyne, and Stedman, 1966). These authors reported a preliminary k_{N_2} value of $(9.7\pm1.4) \times 10^{-32}$ cm^6 $molec^{-2}$ s^{-1} at 293K. However, there is some indication that the above results might have been as much as 15% too low due to a systematic error in their technique (Watson, NBS Rate Constant Review). The NBS value of k_a of $1.1\pm.2 \times 10^{-31}$ is in very good agreement with our value of $(1.24\ .12) \times 10^{-31}$ cm^6 $molec^{-2}$ s^{-1} for $M=N_2$. At the present time, therefore, it appears that the new measurement of k_a should not have any impact on existing modelling efforts on either the ClO_x or NO_x catalytic cycles. It should be noted, however, that the negative temperature dependence (E_a = +2348 cal/molec) for reaction (a) will result in a 220K rate constant ~four times larger than that at 300K.

$$\text{(ii)}\quad Cl(^2P_{3/2}) + NO_2 \xrightarrow{M} ClNO_2 \ .$$

Figure 2 shows a plot of k_b (at 298K) as a function of pressure for the third body gases, N_2 and He . Both plots are linear up to 50 torr of N_2 and 200 torr He . At 200 torr of N_2 , the value of k_b is ∿5% lower than that extrapolated from the lower pressure value of k_b ; similarly, the 500 torr He value is ∿16% lower than that extrapolated from the low pressure data. These trends indicate that this reaction could very well be in the high pressure fall-off regime above ∿100 torr of N_2 or 200 torr of He . This would indicate that under stratospheric conditions, the reaction is termolecular.

Only one value of k_b has been reported in the literature (Clyne and White, 1974). These authors have listed a provisional value for k_b of 7.2×10^{-31} cm^6 $molec^{-2}$ s^{-1} . Our value for k_b $(M=N_2)$ is two times higher than that reported by Clyne and White. Since reaction (b) also has a negative temperature dependence of 980±100 cal/mole, at stratospheric temperatures k_b would be six times higher than the value used in some stratospheric models. The latter situation would be true in those cases where a particular model had assumed no temperature dependence for k_b . It is expected that the measured change in the value of k_b should have a calculable effect on existing stratospheric models. Our best estimates, at the moment, are in the range of a 3-10% lowering of the efficiency of the overall catalytic ozone destruction cycle.

$$\text{(iii)}\quad Cl(^2P_{3/2}) + SO_2 \xrightarrow{M} ClSO_2 \quad .$$

Our investigation of reaction (c) has shown that this process is sufficiently slow that even at very high stratospheric concentrations of SO_2 (as reported by Sagawa and Itoh), it is very unlikely that this reaction could act as an effective chemical trapping process for chlorine atoms.

TABLE I

$$Cl + NO \xrightarrow{M} ClNO$$

Temperature in K	Pressure in Torr	Gas	k_{bi} in cm^3 $molec^{-1}s^{-1}$	k_{ter} in cm^6 $molec^{-2}s^{-1}$	
298	5	N_2	2.2×10^{-14}	1.24×10^{-31}	
	15	N_2	$(6.08\pm0.45)\times10^{-14}$		
	30	N_2	$(1.16\pm0.08)\times10^{-13}$		
	50	N_2	$(1.99\pm0.07)\times10^{-13}$		
	75	N_2	30×10^{-13}		
298	15	He	$(4.37\pm0.41)\times10^{-14}$	8.98×10^{-32}	
	50	He	1.45×10^{-13}		
	100	He	$(2.95\pm0.28)\times10^{-13}$		
	200	He	$(5.78\pm0.29)\times10^{-13}$		
240	80.5	He	$(7.30\pm0.58)\times10^{-13}$	2.27×10^{-31}	$k = 1.63\times10^{-33}\exp(1186/T)$
270	90.5	He	$(4.17\pm0.28)\times10^{-13}$	1.30×10^{-31}	
298	100	He	$(2.95\pm.28)\times10^{-13}$	8.98×10^{-32}	
350	117.5	He	$(1.53\pm.10)\times10^{-13}$	4.75×10^{-32}	

TABLE II

$$Cl + NO_2 \xrightarrow{M} ClNO_2$$

Temperature in K	Pressure in Torr	Gas	k_{bi} in cm^3 $molec^{-1}s^{-1}$	k_{ter} in cm^6 $molec^{-2}s^{-1}$	
298	5	N_2	$(2.98\pm0.10)\times10^{-13}$	1.42×10^{-30}	If only the first three pressures are used, $k_{ter}=1.54\times10^{-30}$ cm^6 $molecule^{-2}s^{-1}$
	15	N_2	$(7.80\pm.31)\times10^{-13}$		
	50	N_2	$(2.53\pm.10)\times10^{-12}$		
	200	N_2	$(9.22\pm.47)\times10^{-12}$		
298	15	He	4.0×10^{-13}	5.52×10^{-31}	If only the first four pressures are used, $k_{ter}=6.75\times10^{-31}$ cm^6 $molecule^{-1}s^{-1}$
	50	He	$(1.23\pm.007)\times10^{-12}$		
	100	He	$(2.19\pm.12)\times10^{-12}$		
	200	He	$(4.45\pm.23)\times10^{-12}$		
	500	He	$(9.10\pm0.18)\times10^{-12}$		
240	15	He	7.58×10^{-13}	1.27×10^{-30}	$k_{b(He)}=1.45\times10^{-31}\exp(529/T)$
270	15	He	5.92×10^{-13}	1.11×10^{-30}	
298	15	He	4.0×10^{-13}	8.28×10^{-31}	
350	15	He	2.69×10^{-13}	6.54×10^{-31}	
240	15	N_2	$(1.40\pm0.08)\times10^{-12}$	2.33×10^{-30}	$k_{b(N_2)}=3.42\times10^{-31}\exp(460/T)$
270	15	N_2	$(9.98\pm0.82)\times10^{-13}$	1.87×10^{-30}	
298	15	N_2	$(7.80\pm0.31)\times10^{-13}$	1.62×10^{-30}	
350	15	N_2	$(5.22\pm0.22)\times10^{-13}$	1.27×10^{-30}	

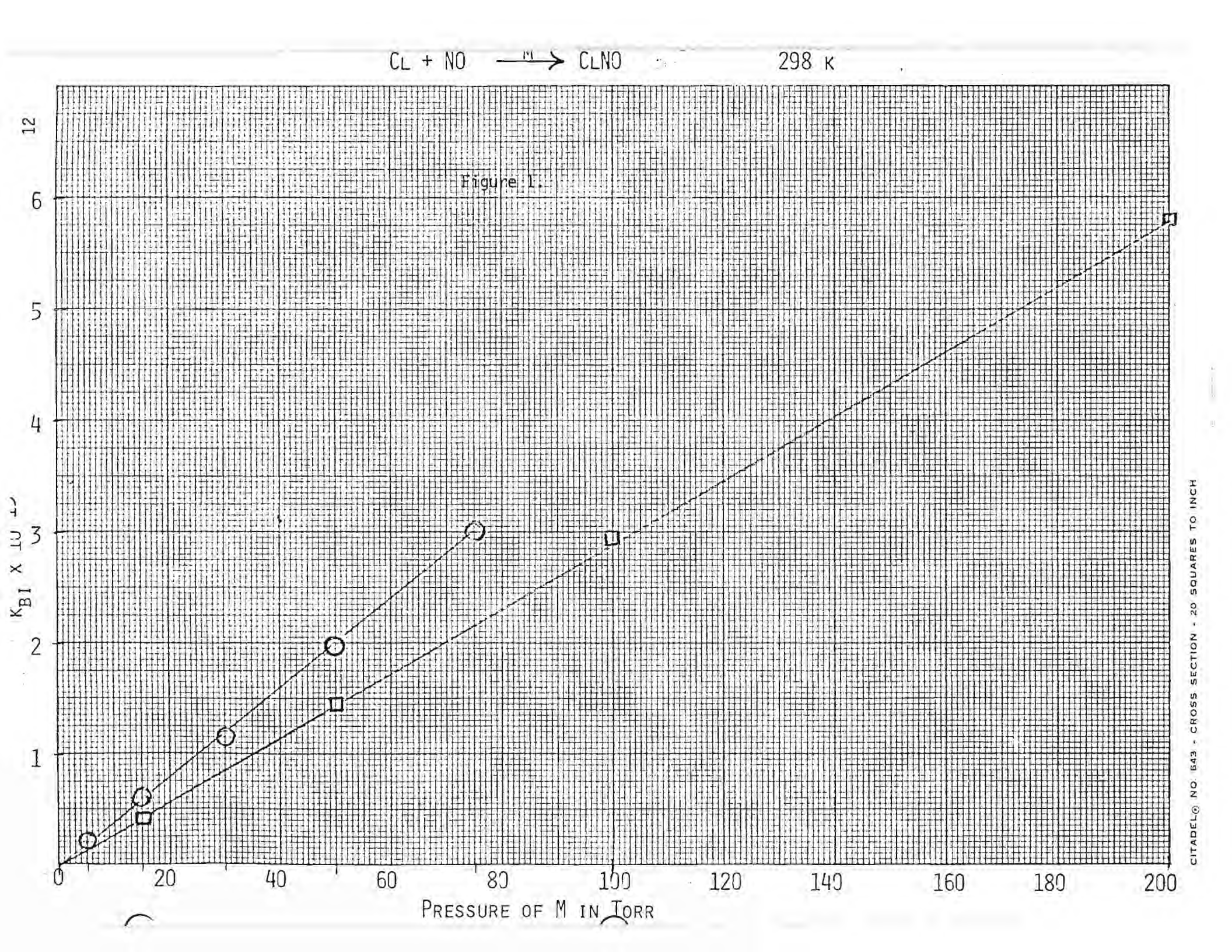
Cl + NO —M→ ClNO
298 K
Figure 1.
12
6
5
4
3
2
1
K_{BI} x 10 ^{17}
0
20
40
60
80
100
120
140
160
180
200
Pressure of M in Torr
CITADEL© NO 643 - CROSS SECTION - 20 SQUARES TO INCH

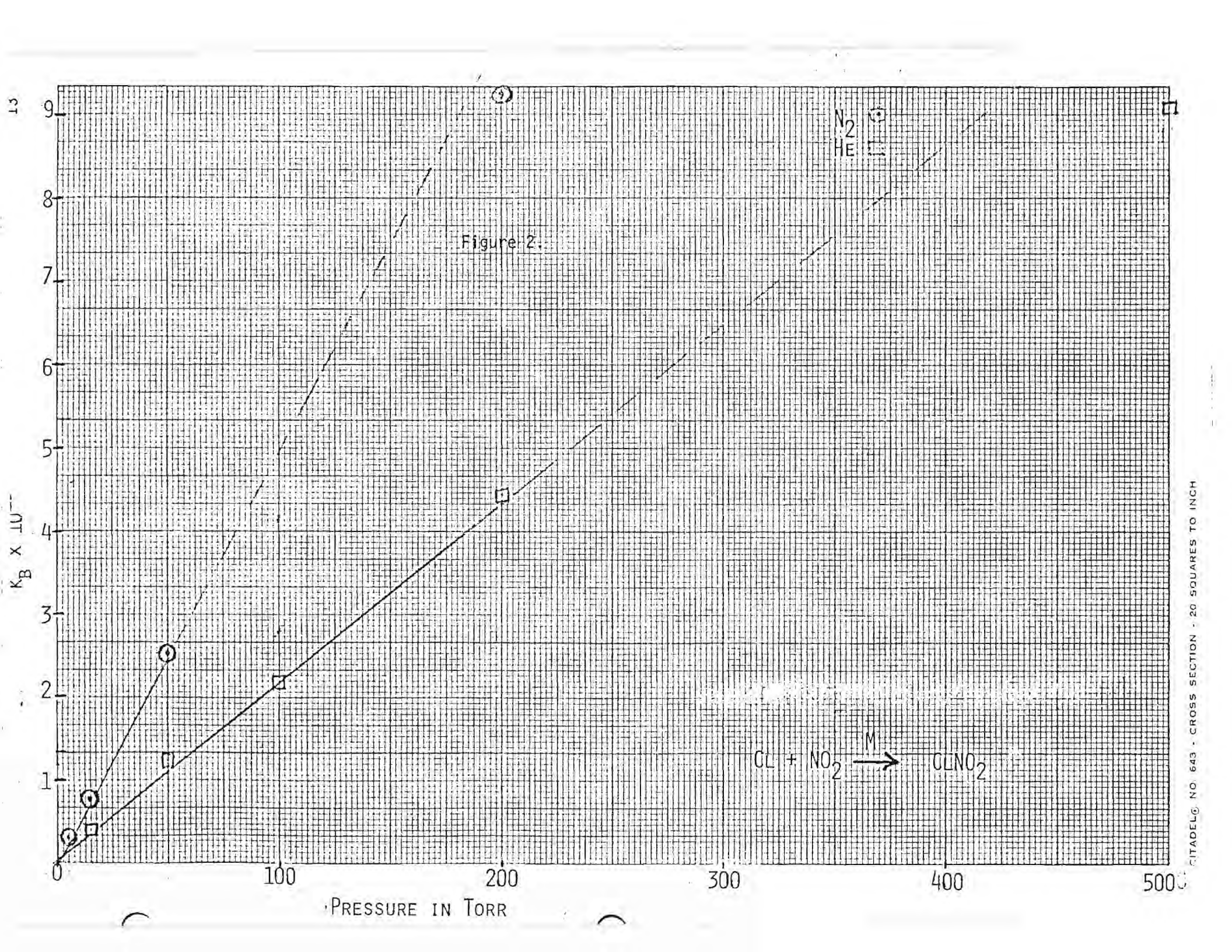
Figure 2.
N_2
He
$Cl + NO_2 \xrightarrow{M} ClNO_2$
$K_B \times 10^{-}$
Pressure in Torr
0
100
200
300
400
500
1
2
3
4
5
6
7
8
9
CITADEL® NO. 643 - CROSS SECTION - 20 SQUARES TO INCH

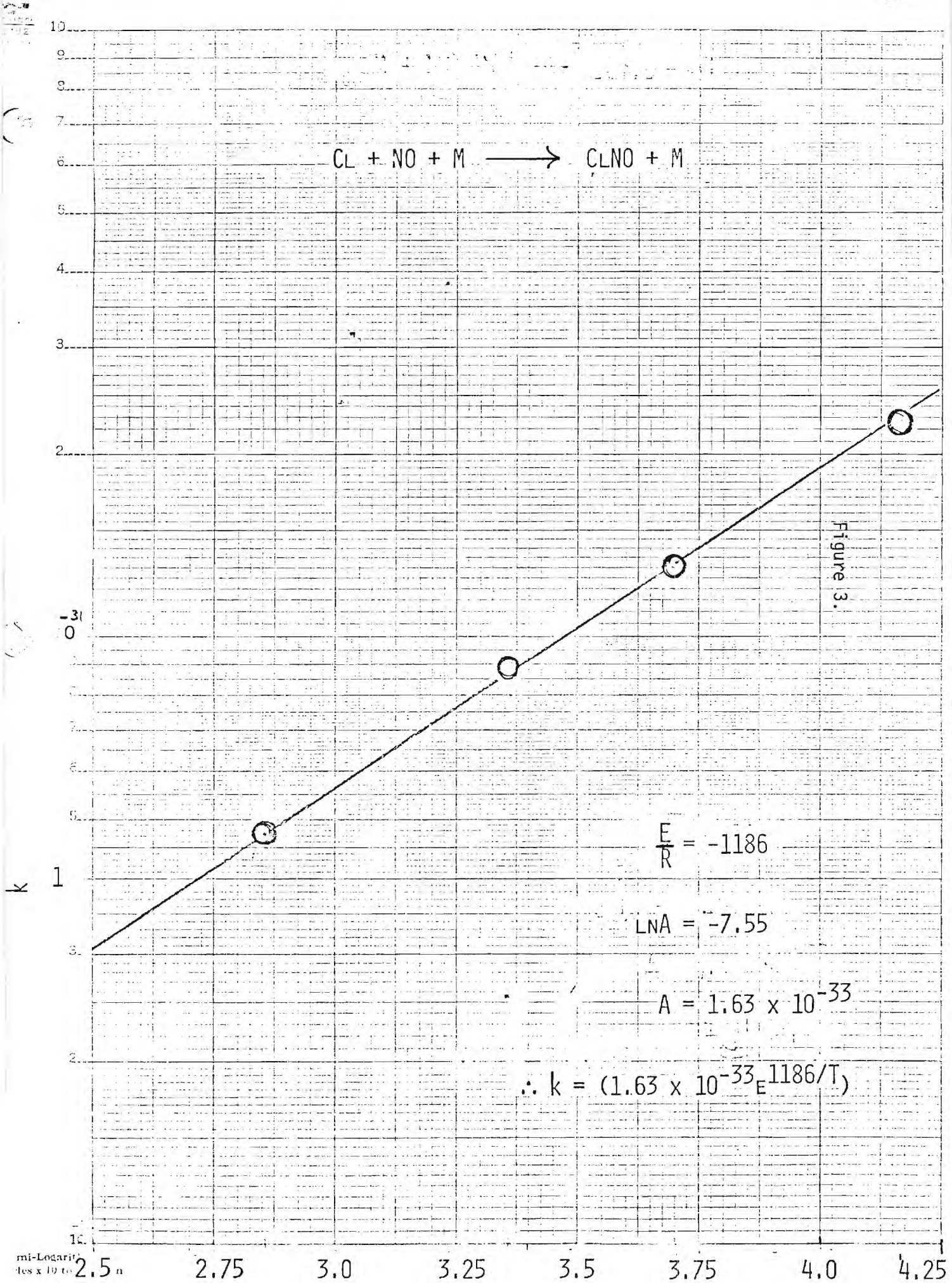

Figure 3.

$\frac{E}{R} = -1186$

$LNA = -7.55$

$A = 1.63 \times 10^{-33}$

$\therefore k = (1.63 \times 10^{-33} E^{1186/T})$

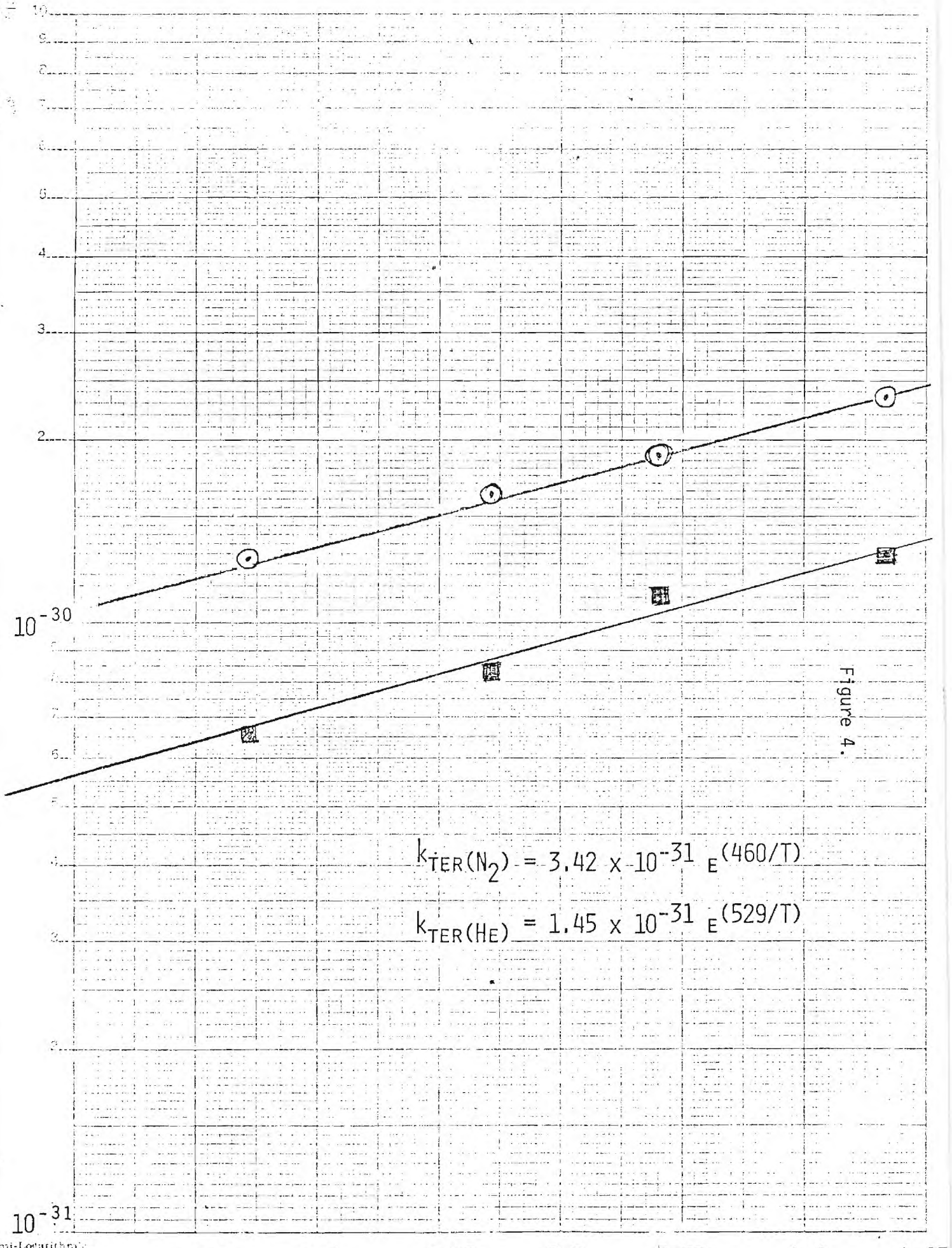

Figure 4.

$$k_{TER(N_2)} = 3.42 \times 10^{-31} e^{(460/T)}$$

$$k_{TER(He)} = 1.45 \times 10^{-31} e^{(529/T)}$$

REFERENCES

Clark, T.C., M. A. Clyne, and D.H. Stedman, Trans. Far. Soc., 62, 3354, 1966.

Clyne, M.A.A. and I.F. White, to be published (1974), see Watson's review.

Davis, D.D., R. Schiff, and S. Fischer, J. Chem. Phys., 61, 2213, 1974.

Davis, D.D., R. Huie, J. Herron, J.W. Braun, and M. Kurylo, J. Chem. Phys., 56, 4868, 1972.

Davis, D.D., and R.B. Klemm, Int. J. Chem. Kinet., 4, 367, 1972.

Watson, R.T., G. Machado, S. Fischer, and D.D. Davis, J. Chem. Phys., 65, 2126, 1976.

Watson, R.T., Chemical Kinetics Data Survey NBSIR-74-516.

SECTION B

Absolute Absorption Cross-sections of ClO

High Resolution Absorption Cross Sections for the $A^2\Pi - X^2\Pi$ System of ClO

1. Introduction

The ClO molecule is believed to be an important intermediate in the catalytic destruction of ozone by chlorine-containing compounds.[1] A quantitative assessment of ozone depletion resulting from the injection of large amounts of chlorofluorocarbons into the atmosphere requires a knowledge of both numerous ClO formation-destruction rates and stratospheric ClO concentrations. While accurate rate constants for many of the significant kinetic processes are now available,[2] the determination of stratospheric concentration profiles remains a difficult problem. Interest in UV absorption as a potential monitoring technique has increased considerably since recent attempts to observe ClO fluorescence proved unsuccessful.[3,4] However, before application of this technique can become a reality, absorption cross sections must be known accurately. At present, only low resolution data is available.[5,6] High resolution cross sections are needed for several reasons: (1) high resolution measurements are inherently more sensitive since the sample can be probed only where the absorption cross section is maximized, (2) only in the high resolution limit is the measured apparent cross section (i.e., the cross section computed under the assumption that all ClO molecules can absorb the incident radiation) independent of bandwidth, and (3) for monitoring purposes, high resolution makes it possible to distinguish ClO absorption from background O_3 absorption by simply tuning the spectroscopic probe on and off a line. In this paper, we report ClO absorption cross sections which were measured using a frequency doubled tunable dye laser with a bandwith of .015Å (much narrower than the width of a single spectral line) as the spectroscopic probe.

2. ClO Spectroscopy

The spectrum of ClO $A^2\Pi_i - X^2\Pi_i$ was first observed in emission from flames by Pannetier and Gaydon[7] and in absorption by Porter.[8] Vibrational and rotational assignments for the $A^2\Pi_i$ state were first given by Durie and Ramsay.[9] The recent work of Coxon and Ramsay[10,11] has resulted in a correction of the vibrational assignments, more accurate line frequencies, and estimates of linewidths. The reported linewidths are constant within a band but vary from band to band over a range of 0.3 to 5cm^{-1}, indicating that predissociation occurs from all vibrational levels with lifetimes in the picosecond range (thus explaining the inability of investigators to observe ClO fluorescence[3, 4]. For our initial experiments, we have chosen to study the $A^2\Pi_{3/2} - X^2\Pi_{3/2}$ 9-0 band. Although the 11-0 band has the largest Franck-Condon factor,[12] the 9-0 band is expected to have the largest peak absorptions and best resolved spectrum; this is because the P(J) and R(J+3) lines exactly overlap (to within .005Å), resulting in a spectrum which exhibits half the expected number of lines but double the expected peak intensities. Furthermore, overlap of the weaker $A^2\Pi_{1/2} - X^2\Pi_{1/2}$ system with the 9-0 band is minimal. Over the spectral range 2822-2834Å, only a few weak, high J lines of the $A^2\Pi_{1/2} - X^2\Pi_{1/2}$ 9-0 band are found; the intensities of these lines are negligible compared to the $A^2\Pi_{3/2} - X^2\Pi_{3/2}$ 9-0 line intensities. Since the spacing between adjacent rotational lines increases with increasing J, optimum resolution is obtained when studying high J levels. However, for J" > 12.5 (at 300°K), line intensities decrease with increasing J due to diminishing population in the ground state J" levels. As a compromise between absorption intensity and resolution, we have focussed most of our attention on the R(19.5-21.5), P(16.5-18.5) lines. For completeness, measurements have also been made in the bandhead region.

3. Experimental

The experimental apparatus is shown schematically in Figure 1. It consists of two major components--a flow system for producing a known concentration of ClO and a laser system for producing a narrow line spectroscopic probe.

ClO was prepared by the reaction

$$Cl + O_3 \rightarrow ClO + O_2 . \qquad (1)$$

Chlorine atoms were generated by passing a Cl_2/He mixture through a microwave discharge, while ozone was generated using a commercial ozonizer and stored at 196°K in a U-tube packed with silica gel. Ozone (95% O_3, 5% O_2) was admitted to the flow tube through a movable injector which was positioned 2cm upstream from the monitoring region to assure complete mixing of gases. The O_3 concentration in the absence of Cl atoms was monitored by absorption of the 2537Å line from a mercury pen-ray lamp. In the presence of an excess of Cl atoms, reaction (1) proceeds very quickly to completion ($k \sim 10^{-11}$ cc/molec-sec), resulting in a ClO concentration equal to the initial O_3 concentration. Experiments were always performed with Cl atoms in excess to avoid overlapping absorption by O_3 and ClOO. The ClOO molecule is formed in secondary reactions but itself reacts so quickly with Cl that, if Cl is in excess, the steady state concentration of ClOO is negligible. Two criteria were satisfied simultaneously to prove that Cl atoms were in excess: (1) absorption at 2537Å falls by a factor of 2.7 when Cl atoms are added to the O_3 (2.7 is the ratio of the absorption cross sections at 2537Å for O_3 and ClO[13-15]) and (2) the chlorine afterglow, which results from atom-atom radiative recombination, is observed downstream from the observation region. To insure that the ClO concentration remained constant during an experiment, absorption at 2537Å was monitored continuously. The typical operating pressure in the flow tube was 1.2 torr.

The ClO concentration was expected to decay down the flow tube as a result of the reaction

$$ClO + ClO \xrightarrow{k_1} Cl_2 + O_2 \qquad (2)$$
$$\xrightarrow{k_2} ClOO + Cl \quad ,$$

whose total rate constant $(k_1 + k_2)$ is $2.5 \times 10^{-14} cm^3/molec\text{-}sec.$[2] Experiments in which ClO absorption was measured at varying distances from the formation region confirmed that reaction (2) controls the ClO gradient. For most experiments, the laser probe was positioned 4cm downstream from the pen-ray lamp. With our linear flow rate of $\sim$ 400 cm/sec and an initial ClO concentration of 1×10^{15} molec/cc, reaction (2) resulted in a 25% decay over 4 cm. Since ClO was probed more than .01 sec after its formation, total relaxation was virtually assured and absorption due to "hot" bands should have been negligible. Absorption measurements were carried out at ClO concentrations which varied from 3.8×10^{14} to 1.2×10^{15} molec/cm^3. The amount of absorption was found to scale linearly with concentration, thus indicating that no product of ClO + ClO chemistry could be an interfering absorber. To further test the possibility that an impurity or product of secondary chemistry could absorb radiation in the same wavelength region as ClO, an experiment was performed where NO was added to the flow through the secondary inlet. NO consumes ClO very quickly via the raction

$$NO + ClO \rightarrow NO_2 + Cl \quad , \qquad (3)$$

so in the presence of excess NO, no ClO absorption should have been observed downstream at the laser probe. In fact, when ClO was titrated with NO, no absorption was observed. Even though this result is not completely definitive

(i.e., it is possible that some species which also reacts quickly with NO could still be an interfering absorber), it strongly suggests that interfering absorptions were not a problem.

The frequency doubled tunable dye laser is described in detail elsewhere.[16] The tuning elements were three air-gap Fabry-Perot etalons. Laser wavelengths and line profiles were measured with a SPEX 3/4 meter monochromator in fourth order. The monochromator was calibrated using several iron lines in the spectral region 2800-2850Å; the wavelength measurements are estimated to be accurate to ±.1Å. The laser spectral profiles showed a strong line containing >95% of the total intensity with a weak satellite .2Å on one side of the main line. The linewidth was too narrow to measure with the monochromator, but was estimated by pressure tuning through an OH absorption line (doppler width = .012Å) and observing the fluorescence signal as a function of pressure. The laser linewidth was found to ∿ .015Å.

To obtain peak absorptions of 10-15% at ClO concentrations of 1×10^{15} molec/cm^3, a four pass absorption path was employed. The path length was determined to be 20.6cm by measuring the absorption resulting from known amounts of added Cl_2 and O_3. The incident laser intensity was measured by deflecting a few percent of the incoming beam to a photodiode while the transmitted intensity was measured by a second photodiode. The photodiode signals were fed into different channels of a gated charge integrator for signal averaging. A single data point was obtained by measuring the ratio of incident to transmitted laser power with ozone turned off (I_0), then with ozone turned on (I), then again with ozone off (to check for drift in I_0). About 3000 laser pulses (pulse rate = 10 sec^{-1}) were averaged to obtain each data point. Both photodiodes were carefully tested for saturation by measuring

the absorption resulting from known amounts of Cl_2 in a cell of known path length; no evidence for saturation was found. Laser power and beam spatial profile measurements were carried out to assess the importance of bleaching -- a phenomenon which occurs when the population of absorbers is significantly depleted due to absorption from an intense laser beam. It was concluded from these measurements that the reduction in measured absorption resulting from bleaching was negligible.

4. Results and Discussion

Absolute apparent absorption cross sections are plotted versus wavelength in Figure 2. The solid line in the 2829-2831Å region represents a "visual" average of all the experimental data in that spectral region. The 2σ error in the reported cross sections is typically $\pm 20\%$, with the ClO concentration measurement and (particularly in the case of weaker absorptions) the uncertainty in I/I_0 being the principal sources of error.

Two interesting aspects of the data in the 2829-2831Å region are the appearance of an unassigned peak at 2830.6Å and the overall lack of resolution. Neither of these features was expected based on the reported ^{35}ClO spectrum.[10] No rotational analysis of ^{37}ClO has been carried out, but positions of the ^{37}ClO bandheads relative to the corresponding ^{35}ClO bandheads have been reported by Briggs.[18] Using Briggs' isotope shifts and an approximate ^{37}ClO rotational constant calculated from the reported ^{35}ClO rotational constant and the ratio of reduced masses, we have calculated ^{37}ClO line positions. Considering the isotopic abundances (24.5% ^{37}ClO, 75.5% ^{35}ClO) and assuming a thermal population distribution (300°K) of ground state rotational levels, it is estimated that $\sim$ 35% of the total absorption intensity in the 2829-2831Å region is due to ^{37}ClO. The exact appearance of the spectrum depends not only

upon line positions and relative intensities, but also upon linewidths. Estimates for ^{35}ClO linewidths are available but ^{37}ClO linewidths are unknown. For the purpose of simulating the spectrum, we have assumed that the ^{37}ClO linewidths are equal to those for ^{35}ClO. In Figure 3, spectra which were calculated assuming Lorentzian lineshapes and linewidths of .20Å and .32Å respectively (the ^{35}ClO linewidth reported by Coxon and Ramsay is .17Å[10]), are compared with the experimental spectrum. Due to the uncertainties in ClO line positions and linewidths, the simulated spectra are very approximate in nature. Nonetheless, some useful qualitative conclusions can be drawn: (1) a baseline resolved spectrum is not feasible, (2) the unassigned spectral feature could be a ^{37}ClO line, and (3) when compared with experimental data, the simulated spectra suggest that the ^{35}ClO linewidth could be somewhat wider than estimated by Coxon and Ramsay.[10]

Examination of the simulated spectra suggests that, at each of the three main peaks, a good estimate for the fraction of intensity which is attributable to ^{35}ClO is 85 ±5%. This fraction of the total cross section is partitioned between the R(J"+3) and P(J") lines. The ratio of apparent cross sections for the two overlapped lines is given by

$$\frac{\sigma^{R}_{J"+3_{app}}}{\sigma^{P}_{J"_{app}}} = \frac{S^{R}_{J"+3}}{S^{P}_{J"}} e^{-\Delta E/KT} , \qquad (4)$$

where $S^{P}_{J"}$ is the line strength of the P(J") line[19] and $\Delta E \equiv E_{J"+3}-E_{J"}$. The real cross section is the apparent cross section divided by the fraction of the total $X^2\Pi_i$ population found in the level from which absorption occurs. Isotopic abundances, spin-orbit splitting (A = 318cm^{-1} [20]), and the

rotational and vibrational state population distributions have been considered in computing this fraction. Apparent and real cross sections for the R(19.5-21.5) and P(16.5-18.5) lines are given in Table 1.

It has been observed that the optimum wavelength region for stratospheric measurements of ClO by absorption is $\sim$3000Å (3-0 and 4-0 bands), even though the absorption cross sections in this wavelength region are rather small.[6] This is because Rayleigh scattering and interfering absorption by ozone become progressively more important at shorter wavelengths. Thus, our future efforts at measuring ClO absorption cross sections will be focussed on the 3-0 and 4-0 bands; a more complete set of measurements on the 9-0 band is also anticipated.

REFERENCES

(1) M. J. Molina and F. S. Rowland, Nature 249, 810 (1974).

(2) R. T. Watson, "Rate Constants of ClO_x of Atmospheric Interest", Chemical Kinetics Data Survey, NBSIR 74-516 (1974).

(3) P. Hogan, R. T. Watson, and D. D. Davis, unpublished results.

(4) M. A. A. Clyne, I. S. McDermid, and A. H. Curran, J. Photochem 5, 201 (1976).

(5) M. A. A. Clyne and J. A. Coxon, Proc. Roy. Soc. A(303), 207 (1968).

(6) P. Rigand, B. Leroy, G. LeBras, G. Poulet, J. L. Jourdain, and J. Combourieu, Chem. Phys. Lett. 46, 161 (1977).

(7) G. Pannetier and A. G. Gaydon, Nature 161, 241 (1948).

(8) G. Porter, Discuss. Far. Soc. 9, 60 (1950).

(9) R. A. Durie and D. A. Ramsay, Can. J. Phys. 36, 35 (1958).

(10) J. A. Coxon and D. A. Ramsay, Can. J. Phys. 54, 1034 (1976).

(11) J. A. Coxon, J. Photochem 5, 337 (1976).

(12) J. A. Coxon, to be published.

(13) W. B. DeMore and O. Raper, J. Phys. Chem. 68, 412 (1964).

(14) M. Griggs, J. Chem. Phys. 49, 857 (1968).

(15) H. S. Johnston, E. D. Morris, Jr., and Van der Bogaerde, J. Amer. Chem. Soc. 91, 7712 (1969).

(16) A. Moriarty, W. Heaps, and D. D. Davis, Opt. Comm. 16, 324 (1976).

(17) D. D. Davis, W. Heaps, D. L. Philen, T. McGee, A. C. Nelson, and P. H. Wine, App. Optics, to be published.

(18) A. G. Briggs, Nature Phys. Sci. 239, 13 (1972).

(19) G. Herzberg, "Spectra of Diatomic Molecules," 2nd Edition, Van Nostrand Reinhold Co., (1950).

(20) N. Basco and R. D. Morse, J. Mol. Spectrosc. 45, 35 (1973).

Table 1. Absolute peak absorption cross sections for individual lines of the $^{35}ClO\ A^2\Pi_{3/2} - X^2\Pi_{3/2}$ 9-0 band ($T = 300^oK$). Accuracy is $\pm 25\%$. Precision is $\pm 10\%$.

Line	$\sigma_{app}(10^{-18}cm^2)$	$\sigma(10^{-17}cm^2)$
R(19.5)	2.5_5	10.6
R(20.5)	2.3	10.3
R(21.5)	1.9	9.2
P(16.5)	2.8_5	10.0
P(17.5)	2.6	9.6
P(18.5)	2.2	8.6

Figure Captions

Figure 1. Schematic of experimental apparatus.

Figure 2. Experimental apparent absorption cross sections for the ClO $A^2\Pi_{3/2} - X^2\Pi_{3/2}$ 9-0 band. o: (ClO) = 1.2×10^{15} molec/cc; •: (ClO) = 1.0×10^{15} molec/cc; x: (ClO) = 3.8×10^{14} molec/cc; ——— : "visual average" spectrum.

Figure 3. Comparison of simulated ClO spectra with the experimental spectrum. The more intense sequence of lines in the simulated spectra represent ^{35}ClO; the weaker sequence of lines represent ^{37}ClO. A: experimental spectrum; B: all (pairs of) lines assumed to have .20Å linewidth; C: all (pairs of) lines assumed to have .32Å linewidth.

FIGURE

29

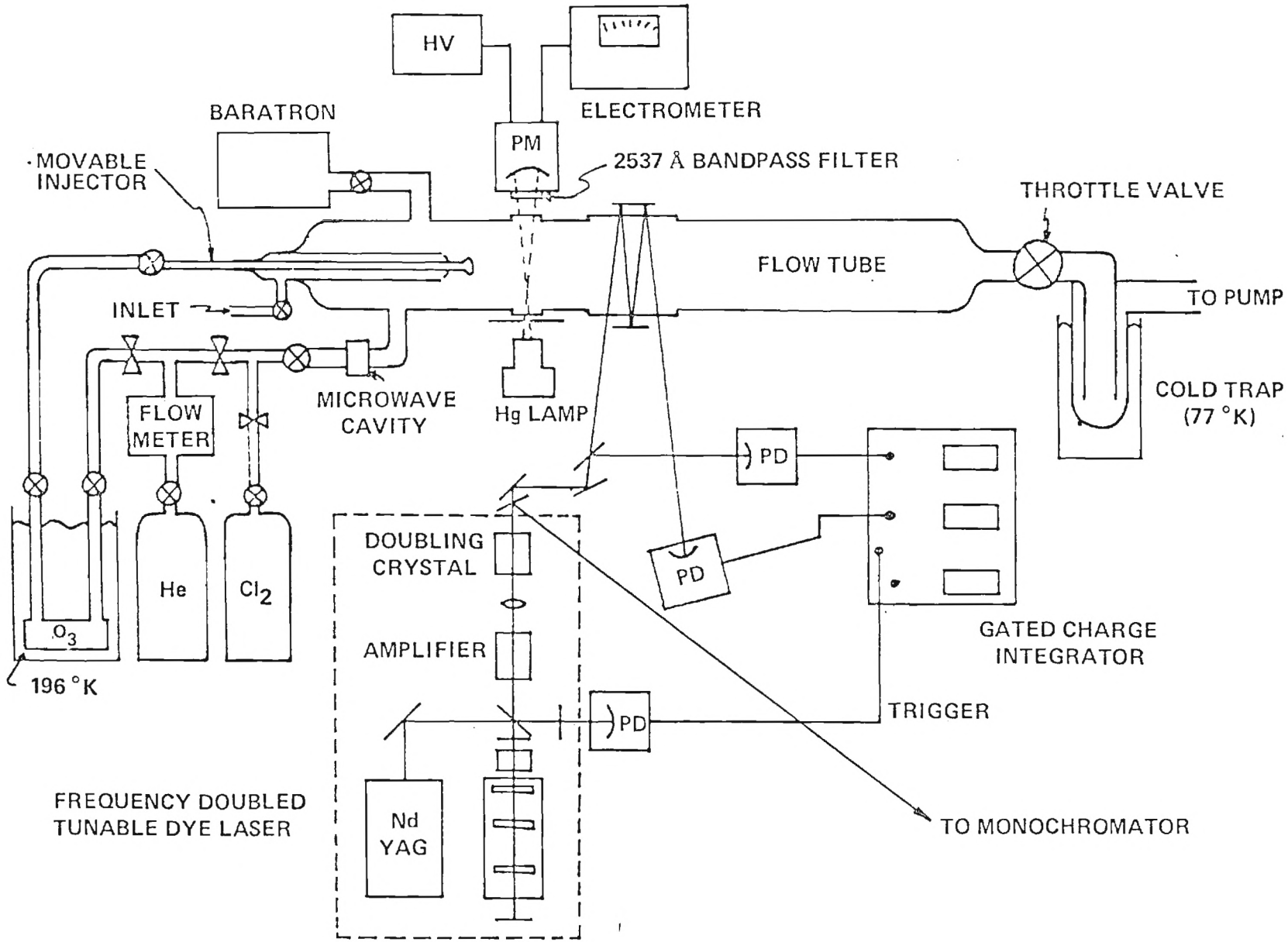
HV
ELECTROMETER
BARATRON
PM
2537 Å BANDPASS FILTER
MOVABLE INJECTOR
THROTTLE VALVE
FLOW TUBE
INLET
TO PUMP
COLD TRAP (77 °K)
FLOW METER
MICROWAVE CAVITY
Hg LAMP
PD
DOUBLING CRYSTAL
PD
He
Cl_2
O_3
AMPLIFIER
GATED CHARGE INTEGRATOR
196 °K
TRIGGER
PD
FREQUENCY DOUBLED TUNABLE DYE LASER
Nd YAG
TO MONOCHROMATOR

FIGURE 2

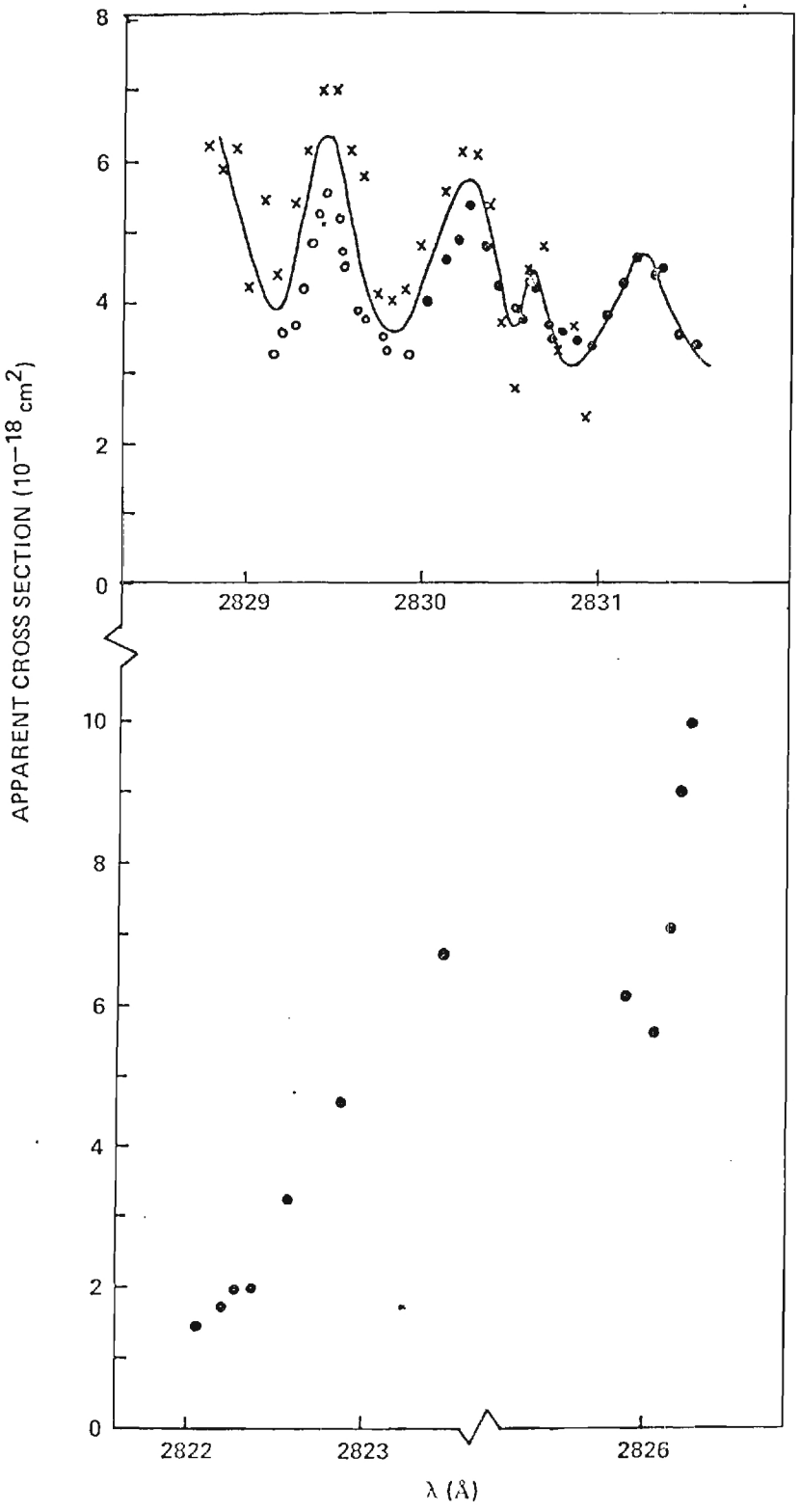
APPARENT CROSS SECTION (10^{-18} cm^2)
λ (Å)
0
2
4
6
8
10
2822
2823
2826
2829
2830
2831

FIGURE